EXPANDED SPACE MAPPING EM BASED DESIGN FRAMEWORK EXPLOITING PREASSIGNED PARAMETERS

John W. Bandler, *Fellow*, *IEEE,* Mostafa A. Ismail, *Student Member, IEEE* and
José E. Rayas-Sánchez, *Senior Member*, *IEEE*

Keywords Space mapping, preassigned parameters, design automation, EM optimization, microwave circuits, microstrip filters, optimization methods

Abstract We present a novel design framework for microwave circuits. We calibrate coarse models (circuit based models) to align with fine models (full wave EM simulations) by allowing some preassigned parameters (which are not used in optimization) to change in some components of the coarse model. We refer to those components as "designated" and we present a method based on sensitivity analysis to identify them. Our Expanded Space Mapping Design Framework (ESMDF) algorithm calibrates the coarse model iteratively by extracting the preassigned parameters of the designated components. It establishes a mapping from optimizable to preassigned parameters. This mapping is sparse and is established with few fine model simulations. The algorithm updates the mapping and terminates if relevant stopping criteria are satisfied. Software implementation as well as interfacing with commercial EM simulators are addressed. We illustrate our approach through three microstrip design examples.

I. INTRODUCTION

The concept of calibrating coarse models (computationally fast circuit based models) to align

---

This work was supported in part by the Natural Sciences and Engineering Research Council of Canada under Grants OGP0007239 and STR234854-00, through the Micronet Network of Centres of Excellence and Bandler Corporation. M.A. Ismail is supported by a Nortel Networks Ontario Graduate Scholarship in Science and Technology. J.E. Rayas-Sánchez was supported by an Ontario Graduate Scholarship, as well as by ITESO (Instituto Tecnológico y de Estudios Superiores de Occidente, Mexico).

J.W. Bandler, M.A. Ismail and J.E. Rayas-Sánchez are with the Simulation Optimization Systems Research Laboratory and the Department of Electrical and Computer Engineering, McMaster University, Hamilton, Ontario, Canada L8S 4K1.

J.W. Bandler is also with Bandler Corporation, P.O. Box 8083, Dundas, Ontario, Canada L9H 5E7.

with fine models (typically CPU intensive full wave EM simulations) in microwave circuit design has been exploited by several authors [1 , 2, 3, 4]. In [1, 2, 3], this calibration is performed through a mapping between the optimizable parameters of the coarse model and those of the fine model such that the corresponding responses match. This mapping is iteratively updated. In [4], the coarse model is calibrated with the fine model by adding circuit components to nonadjacent individual coarse model elements. The values of these components are updated iteratively.

Here, we expand the original space mapping technique [1]. We calibrate the coarse model by allowing "preassigned" parameters to change in some coarse model components. Examples of preassigned parameters are dielectric constant and substrate height in microstrip structures. We assume that the coarse model consists of several components such as transmission lines, junctions, etc. We decompose the coarse model into two sets of components. We allow the preassigned parameters to change in the first set and keep them intact in the second set. In Section III we present a method based on sensitivity analysis to perform this decomposition.

For example, the coarse model of the three-section microstrip transformer in Fig. 1(b) consists of five components: three microstrip lines and two step junctions. The transmission line lengths and widths (Fig. 1(a)) are the optimizable parameters. The preassigned parameters are the substrate height H and the dielectric constant ε_r. We choose the three transmission lines in Fig. 1(b) (components 1,3,5) as "designated" components (we will see how in Section III). The coarse model is calibrated to align with the fine model (in this case full wave EM simulations by Sonnet's ***em*** [5]) by tuning H and ε_r of each designated component (transmission line). The dielectric constant and the substrate height of the other components (the two step junctions in Fig. 1(b)) are kept intact. Note that we do not change the preassigned parameters in the fine model.

The ESMDF algorithm calibrates the coarse model by extracting the preassigned parameters such that corresponding responses match. It establishes a mapping from optimizable to preassigned parameters. The resulting mapped coarse model (the coarse model with the mapped preassigned parameters) is then optimized subject to a trust region size. The algorithm terminates if certain relevant stopping criteria are satisfied. Otherwise it starts a new iteration and recalibrates the coarse model by extracting the preassigned parameters and updating the mapping. The trust region size is updated [6, 7, 8] according to the match between the fine and mapped coarse model.

II. BASIC CONCEPTS AND NOTATION

Preassigned Parameter Mapping

Consider a microwave circuit represented by a fine model and a coarse model. We decompose the coarse model into two sets of components: a Set A of "designated" components and Set B. See Fig. 2. In Set A, we allow preassigned parameters to change throughout the design process. In Set B, we keep the preassigned parameters intact. The vector $\boldsymbol{x}_0 \in \Re^{n_0}$ represents the original values of the preassigned parameters. Assume that the total number of coarse model components is N, the number of components in the designated Set A is $m \leq N$ and the set I is defined by

$$I = \{1, 2, \cdots, N\} \tag{1}$$

Let $j_1, j_2, \ldots, j_m \in I$ represent the indices of the components in Set A. The vector of corresponding preassigned parameters

$$\boldsymbol{x} = [\boldsymbol{x}_{j_1}^T \; \boldsymbol{x}_{j_2}^T \ldots \boldsymbol{x}_{j_m}^T]^T \in \Re^{mn_0} \tag{2}$$

where $\boldsymbol{x}_{j_i} \in \Re^{n_0}$, i=1, 2, …, m is the ith designated component. The vector $\boldsymbol{x}_f \in \Re^n$ represents the original optimization variables.

We assume that we can establish a mapping from some elements of $\boldsymbol{x}_f$ to $\boldsymbol{x}$ such that the coarse model aligns with the fine model. This mapping is given by

$$\boldsymbol{x} = \boldsymbol{P}(\boldsymbol{x}_r) : \Re^{n_r} \mapsto \Re^{mn_0} \tag{3}$$

$$\boldsymbol{x}_f = [\boldsymbol{x}_r^T \quad \boldsymbol{x}_s^T]^T \tag{4}$$

Decomposition of $\boldsymbol{x}_f$ into $\boldsymbol{x}_r$ and $\boldsymbol{x}_s$ (introduced and justified by Bandler *et al.* [2] as "partial space mapping") allows a reduction of the mapping $\boldsymbol{P}$. We approximate (3) and consider the difference form

$$\Delta \boldsymbol{x} = \boldsymbol{B}_r \ \Delta \boldsymbol{x}_r \tag{5}$$

where $\boldsymbol{B}_r \in \Re^{(mn_0) \times n_r}$ is a matrix to be determined.

Responses

The vector $\boldsymbol{R}_f(\boldsymbol{x}_f, \Omega) \in \Re^{FL}$ represents a complete set of basic responses of the fine model (such as the real and imaginary parts of the S-parameters) at $\boldsymbol{x}_f$ and over a set of frequencies Ω

$$\boldsymbol{R}_f(\boldsymbol{x}_f, \Omega) = [\boldsymbol{R}_f^T(\boldsymbol{x}_f, \omega_1) \ \ \boldsymbol{R}_f^T(\boldsymbol{x}_f, \omega_2) \cdots \boldsymbol{R}_f^T(\boldsymbol{x}_f, \omega_F)]^T \tag{6a}$$

$$\Omega = \{\omega_1, \omega_2, \cdots, \omega_F\} \tag{6b}$$

The number of those responses is L and the cardinality of Ω is F. $\boldsymbol{R}_c(\boldsymbol{x}_f, \boldsymbol{x}, \Omega) \in \Re^{FL}$ is the corresponding set of responses for the coarse model at $\boldsymbol{x}_f$, for the preassigned $\boldsymbol{x}$ and over Ω. The vectors $\boldsymbol{R}_{fs}(\boldsymbol{x}_f, \Omega)$, $\boldsymbol{R}_{cs}(\boldsymbol{x}_f, \boldsymbol{x}, \Omega) \in \Re^{FM}$ represent specific responses (such as $|S_{11}|$, $|S_{21}|$, etc.) of the fine and coarse model, respectively. The design specifications and hence the objective functions are given in their terms. In this work, we use two sets of frequencies. The first set Ω_p is of cardinality F_p. It is used in the preassigned parameter extraction process. The second set Ω_s is of cardinality F_s. It is used for optimizing the mapped coarse model. Typically, we choose $F_s > F_p$ since we wish to simulate the fine model over the least possible number of frequencies.

Illustrative Example

Consider the microstrip transformer in Fig.1. The source and load impedances are 50 and 150 Ω, respectively. The design specifications are

$$|S_{11}| \leq -20 \text{ dB}, \text{ for } 5 \text{ GHz} \leq \omega \leq 15 \text{ GHz}$$

The fine model is analyzed by Sonnet's ***em*** [5]. The coarse model in Fig. 1(b) is analyzed by OSA90/hope [13]. The optimization variables are the widths and the lengths of the microstrip transmission lines in Fig. 1(a). That is,

$$\boldsymbol{x}_f = [W_1\ W_2\ W_3\ L_1\ L_2\ L_3\ ]^T$$

The preassigned parameters are the dielectric constant ε_r = 9.7 and the substrate height H = 25 mil. Therefore, the vector $\boldsymbol{x}_0$=[25 mil 9.7]^T. The coarse model consists of five components (N=5) as shown in Fig. 1(b). The algorithm applies the coarse model decomposition technique in Section III and chooses the components 1, 3 and 5 as designated. Thus Set A consists of the three transmission lines in Fig. 1(b) and Set B consists of components 2 and 4 (the step junctions). The vector of preassigned parameters (in Set A) is

$$\boldsymbol{x} = [\boldsymbol{x}_1^T\ \boldsymbol{x}_3^T\ \boldsymbol{x}_5^T\ ]^T$$

where $\boldsymbol{x}_i = [\varepsilon_{ri} \quad H_i]^T$, i=1, 3, 5. The vector $\boldsymbol{x}_r$ in (3) is given by

$$\boldsymbol{x}_r = [W_1\ W_2\ W_3\ ]^T$$

The matrix $\boldsymbol{B}_r$ is chosen to have the sparsity structure

$$\boldsymbol{B}_r = \begin{bmatrix} \mathrm{x} & 0 & 0 \\ \mathrm{x} & 0 & 0 \\ 0 & \mathrm{x} & 0 \\ 0 & \mathrm{x} & 0 \\ 0 & 0 & \mathrm{x} \\ 0 & 0 & \mathrm{x} \end{bmatrix}$$

where x denotes a nonzero entry. This structure reflects an association between preassigned parameters and the design parameters of the corresponding component. For example, the preassigned parameters of the first, second and third designated components are functions only of W_1, W_2, and W_3, respectively.

The response vectors $\boldsymbol{R}_{fs}, \boldsymbol{R}_{cs}$ contain $|S_{11}|$. The vectors $\boldsymbol{R}_f, \boldsymbol{R}_c$ contain the real and imaginary parts of S_{11}. Set Ω_s contains 21 evenly spaced frequencies while Ω_p contains 11 evenly spaced frequencies from 5 GHz to 15 GHz.

III. COARSE MODEL DECOMPOSITION

We present a method based on sensitivity analysis to decompose the coarse model components into two sets. Set A contains those for which the response is very sensitive to small changes in preassigned parameter values. Set B contains those for which the response is insensitive to changes in preassigned parameters. The method is summarized in the following steps.

Step 1 For all $i \in I$ in (1) evaluate

$$S_i = \left\| \left(\frac{\partial \boldsymbol{R}_{cs}^T}{\partial \boldsymbol{x}_i} \boldsymbol{D} \right)^T \right\|_F \tag{7}$$

where S_i represents a measure of the sensitivity of the coarse model response to preassigned parameters of the ith component, the matrix $\boldsymbol{D}$ is for scaling and $\| \ \|_F$ denotes Frobenius norm.

Comment The Jacobian in (7) is evaluated by perturbation at $\boldsymbol{x}_i = \boldsymbol{x}_0, i \in I$. The matrix $\boldsymbol{D}$ is diagonal. It consists of the elements of $\boldsymbol{x}_0$. For the microstrip transformer in Fig. 1(b), (see Section II), $\boldsymbol{D}$ = diag {25 mil, 9.7}.

Step 2 Evaluate

$$\hat{S}_i = \frac{S_i}{\max\limits_{j \in I} \{S_j\}}, i \in I \tag{8}$$

Comment For the example in Section II, the values of $\hat{S}_i$ are given in Table I, where we notice that $\boldsymbol{R}_{cs}$ is most sensitive to the first transmission line.

Step 3 Put the ith component in Set A if $\hat{S}_i \geq \beta$ otherwise put it in Set B.

Comment The scalar β is a small positive number less than 1. In our examples β = 0.2. For the microstrip transformer, we place components 1, 3 and 5 in Set A (see Table I) and components 2 and 4 in Set B.

IV. THE ESMDF ALGORITHM

The ESMDF algorithm starts by decomposing the coarse model into two sets of components as shown in Section III. Then it obtains the optimal solution of the coarse model. If the fine model response at that solution satisfies the specifications and (or) is very close to the optimal coarse model response (the coarse model is already very good) the algorithm terminates. Otherwise, the algorithm iteratively calibrates the coarse model by extracting the preassigned parameters at the optimal coarse model solution and updating the matrix $\boldsymbol{B}_r$. At each iteration, the algorithm obtains the optimal solution of the mapped coarse model subject to a certain trust region [6, 8]. This solution is accepted if it results in a reduction in the fine model objective function. The trust region size is adaptively updated according to the relative improvement of the fine model objective function to that of the coarse model. The algorithm terminates if any one of some stopping criteria (to be discussed later) is satisfied. It performs four main tasks: mapped coarse model optimization, extraction of preassigned parameters, checking some stopping criteria and updating the mapping parameters and the trust region size.

Mapped Coarse Model Optimization

A trust region methodology controls the optimization of the mapped coarse model to insure improvement in the fine model objective function. Let $\boldsymbol{h}$ denote the prospective step $\Delta \boldsymbol{x}_f$ and $\boldsymbol{h}_r$ denote the corresponding step $\Delta \boldsymbol{x}_r$. At the ith iteration the algorithm obtains the step $\boldsymbol{h}^{(i)}$ by solving the optimization problem

$$\begin{aligned} \boldsymbol{h}^{(i)} &= \arg \min_{\boldsymbol{h}} U(\boldsymbol{R}_{cs}(\boldsymbol{x}_f^{(i)} + \boldsymbol{h}, \boldsymbol{x}^{(i)} + \boldsymbol{B}_r^{(i)}\ \boldsymbol{h}_r)) \\ &\text{subject to } \ \|\boldsymbol{\Lambda}_i \boldsymbol{h}\| \leq \delta_i \end{aligned} \tag{9}$$

where U is a suitable objective function, δ_i is the trust region radius and the matrix $\boldsymbol{\Lambda}_i$ is for scaling [7]. We set $\boldsymbol{\Lambda}_i$ as a diagonal matrix whose elements are the reciprocal of the elements of $\boldsymbol{x}_f^{(i)}$. Therefore, the trust region radius δ_i represents the maximum allowable relative change in the design variables at the ith iteration. The norm used in (9) is the ℓ_∞ norm. The algorithm decides whether to accept the prospective step $\boldsymbol{h}^{(i)}$:

$$\boldsymbol{x}_f^{(i+1)} = \begin{cases} \boldsymbol{x}_f^{(i)} + \boldsymbol{h}^{(i)} & \text{if } U(\boldsymbol{R}_{fs}(\boldsymbol{x}_f^{(i)} + \boldsymbol{h}^{(i)}, \Omega_p)) < U(\boldsymbol{R}_{fs}(\boldsymbol{x}_f^{(i)}, \Omega_p)) \\ \boldsymbol{x}_f^{(i)} & \text{otherwise} \end{cases} \tag{10}$$

The ith iteration is successful if $\boldsymbol{h}^{(i)}$ results in an improvement in the fine model objective function.

The algorithm updates the trust region radius according to the criteria in [7,8]:

1. If the decrease in the fine model objective function is the same as or better than that of the mapped coarse model we enlarge the trust region.
2. However, if the fine model objective function has increased or if it has decreased but not by as much as predicted by the mapped coarse model we shrink the trust region.
3. Otherwise we leave the trust region unchanged.

Mathematically, we evaluate the relative reduction in the fine model objective function with respect to the corresponding reduction in the mapped coarse model objective function

$$r = \frac{U(\boldsymbol{R}_{fs}(\boldsymbol{x}_f^{(i)}, \Omega_p)) - U(\boldsymbol{R}_{fs}(\boldsymbol{x}_f^{(i+1)}, \Omega_p))}{U(\boldsymbol{R}_{cs}(\boldsymbol{x}_f^{(i)}, \boldsymbol{x}^{(i)}, \Omega_p)) - U(\boldsymbol{R}_{cs}(\boldsymbol{x}_f^{(i+1)}, \boldsymbol{x}^{(i)} + \boldsymbol{B}_r^{(i)}\boldsymbol{h}_r^{(i)}, \Omega_p))} \tag{11}$$

Then we update the trust region radius as follows

$$\delta_{i+1} = \begin{cases} 2\delta_i & \text{if } r > r_1 \\ \delta_i / 3 & \text{if } r < r_2 \\ \delta_i & \text{otherwise} \end{cases} \tag{12}$$

where r_1 and r_2 take the values 0.75 and 0.25 [8].

Stopping Criteria

At the *i*th iteration, the algorithm simulates the fine model at the optimal mapped coarse model solution and stops if one of the following stopping criteria is satisfied.

1. A predefined maximum number of iterations $i_{\max}$ is reached. This puts a limit on the number of fine model evaluations the designer can afford.
2. The algorithm reaches a solution that just satisfies the specifications.
3. The mapped coarse model response is very close to the fine model response

$$\left\| \boldsymbol{R}_{fs}(\boldsymbol{x}_f^{(i)}, \Omega_p) - \boldsymbol{R}_{cs}(\boldsymbol{x}_f^{(i)}, \boldsymbol{x}^{(i-1)} + \boldsymbol{B}_{\boldsymbol{r}}^{(i-1)}\boldsymbol{h}_{\boldsymbol{r}}^{(i)}, \Omega_p) \right\| \le \varepsilon_1 \tag{13}$$

   This criterion indicates that the mapped coarse model is doing an excellent job in predicting the improvement in the fine model within certain accuracy.
4. The solutions obtained in two successive successful iterations are very close [3]

$$\left\| \boldsymbol{x}_f^{(i)} - \boldsymbol{x}_f^{(i\text{-}1)} \right\|_\infty \leq \varepsilon_2 \tag{14}$$

5. The radius of the trust region is very small

$$\delta_i < \delta_{\min} \tag{15}$$

where $\delta_{\min}$ is the smallest allowable trust region radius.

If none of the criteria is satisfied and the solution obtained in (10) is successful the algorithm proceeds to extract the preassigned parameters at the optimal coarse model solution, i.e., the next iteration.

Extraction of Preassigned Parameters

At the *i*th iteration, if the algorithm accepts the prospective step $\boldsymbol{h}^{(i)}$ (10) and the stopping criteria are not satisfied, it extracts the vector of the preassigned parameters $\boldsymbol{x}^{(i+1)}$ corresponding to $\boldsymbol{x}_f^{(i+1)}$

$$\boldsymbol{x}^{(i+1)} = \arg\min_{\boldsymbol{x}} \left\| \boldsymbol{R}_f(\boldsymbol{x}_f^{(i+1)}, \Omega_p) - \boldsymbol{R}_c(\boldsymbol{x}_f^{(i+1)}, \boldsymbol{x}, \Omega_p) \right\| \tag{16}$$

where the norm used in (16) is the Huber norm [9]. The optimization problem (16) may get trapped in a poor local minimum if the coarse and fine model responses are severely misaligned. Possible ways to overcome this is to use frequency mapping [10] or statistical parameter extraction [11]. Here, we present another technique. Instead of solving (16) directly we try to roughly align the responses first. We do that by minimizing the difference between the center frequency and the bandwidth of the coarse and the fine model responses

$$\bar{\boldsymbol{x}} = \arg\min_{\boldsymbol{x}} \left| \mu_f(\boldsymbol{x}_f^{(i+1)}) - \mu_c(\boldsymbol{x}_f^{(i+1)}, \boldsymbol{x}) \right| + \left| \sigma_f(\boldsymbol{x}_f^{(i+1)}) - \sigma_c(\boldsymbol{x}_f^{(i+1)}, \boldsymbol{x}) \right| \tag{17}$$

where $\{\mu_f, \mu_c\}$ and $\{\sigma_f, \sigma_c\}$ are estimates of the center frequencies and bandwidths, respectively, for the fine and coarse model responses (see Appendix A). We use this solution as a starting point to solve (16). If this procedure fails to produce a good match the algorithm uses the statistical parameter extraction approach in [11]. That is it tries to solve (16) from different random starting points until it obtains a good match. From our experience we notice that we need to perform this procedure only in the first iteration. For later iterations it is enough to use the previous solution as a starting point to solve (16).

Updating the Mapping Parameters

After extracting the preassigned parameters at the ith iteration the algorithm updates $\boldsymbol{B}_r$ in (5). In the early iterations we have an underdetermined system. We choose the minimum norm solution to render the preassigned parameters close to their original values. That is, we choose $\boldsymbol{B}_r$ close to **0**. At the ith iteration we have

$$[\Delta\boldsymbol{x}^{(1)}\ \Delta\boldsymbol{x}^{(2)}\cdots\Delta\boldsymbol{x}^{(i)}] = \boldsymbol{B}_r\,[\Delta\boldsymbol{x}_r^{(1)}\ \Delta\boldsymbol{x}_r^{(2)}\cdots\Delta\boldsymbol{x}_r^{(i)}] \tag{18}$$

where

$$\Delta\boldsymbol{x}^{(j)} = \boldsymbol{x}^{(j)} - \boldsymbol{x}^{(j-1)},\ j \in 1,2,\ldots,i \tag{19a}$$

$$\Delta\boldsymbol{x}_r^{(j)} = \boldsymbol{x}_r^{(j)} - \boldsymbol{x}_r^{(j-1)},\ j \in 1,\ 2,\ \ldots,\ i \tag{19b}$$

The vector $\boldsymbol{x}^{(0)}$ contains the original values of the preassigned parameters. When solving (18) for $\boldsymbol{B}_r$ sparsity should be considered. Let $\boldsymbol{b} \in \Re^p$ contain the nonzero elements of $\boldsymbol{B}_r$. By rearranging (18) we can write the linear system as

$$\boldsymbol{y} = \boldsymbol{X}_r\ \boldsymbol{b} \tag{20}$$

where $\boldsymbol{y} = [(\Delta\boldsymbol{x}^{(1)})^T\ (\Delta\boldsymbol{x}^{(2)})^T \cdots (\Delta\boldsymbol{x}^{(i)})^T]^T \in \Re^{m\,n_0\,i}$ and $\boldsymbol{X}_r \in \Re^{m n_0 i \times p}$ is a sparse matrix whose nonzero elements are the elements of $\Delta\boldsymbol{x}_r^{(1)}, \Delta\boldsymbol{x}_r^{(2)}, \cdots \Delta\boldsymbol{x}_r^{(i)}$. The structure of the matrix $\boldsymbol{X}_r$ depends on the sparsity of $\boldsymbol{B}_r$. The solution of (20) is given by

$$\boldsymbol{b} = \boldsymbol{X}_r^+\ \boldsymbol{y} \tag{21}$$

where $\boldsymbol{X}_r^+$ is the pseudoinverse of $\boldsymbol{X}_r$. A Matlab [12] function is written to construct the matrix $\boldsymbol{X}_r$ and the Matlab function pinv is used to evaluate $\boldsymbol{X}_r^+$. The advantage of using the pseudoinverse is that it gives us the minimum norm solution for underdetermined systems.

Summary of the ESMDF Algorithm

Given δ_0 (the initial trust region radius), $\delta_{\min}$, $i_{\max}$, ε_1, ε_2 the algorithm performs the following steps.

Step 1 Decompose the coarse model components into sets A and B as mentioned in Section III. Initialize $i = 0$, $\boldsymbol{B}_r=0$.

Step 2 Optimize the coarse model. Designate the optimal solution $\boldsymbol{x}_f^{(0)}$.

Step 3 Simulate the fine model at $\boldsymbol{x}_f^{(0)}$. Terminate if a stopping criterion is satisfied.

Step 4 Extract the preassigned parameters $\boldsymbol{x}^{(i)}$ by solving (16). Update $\boldsymbol{B}_r$ using (21).

Step 5 Evaluate the prospective step $\boldsymbol{h}^{(i)}$ by optimizing the mapped coarse model (9).

Mark i as a successful iteration if $U(\boldsymbol{R}_{fs}(\boldsymbol{x}_f^{(i)}+\boldsymbol{h}^{(i)},\Omega_p)) < U(\boldsymbol{R}_{fs}(\boldsymbol{x}_f^{(i)},\Omega_p))$.

Set $\boldsymbol{x}_f^{(i+1)}$ according to (10).

Comment When i=0 we disable the trust region, hence δ_0 can be small. For example, 0.05 is used in our design examples.

Step 6 Evaluate r in (11). Update δ from (12). Increment i.

Step 7 If a stopping criterion is satisfied terminate.

Step 8 If the ith iteration is successful go to Step 4, otherwise go to Step 5.

V. SOFTWARE IMPLEMENTATION

The ESMDF algorithm is currently implemented in Matlab™[12]. The user writes a text input file which includes coarse and fine model names and directories, frequency ranges, design specifications, starting point for the optimization variables and other parameters such as the maximum allowable number of fine model simulations and the initial trust region radius. The program outputs the solution process, including plots of the mapped coarse and fine model responses, the objective function, parameter values and $\boldsymbol{B}_r$.

The current implementation drives Sonnet's ***em*** [5] through OSA90/hope [13]. It uses the OSA90/hope optimizers (not Matlab). Driving other EM simulators (with parameterization capability [14]) automatically from within Matlab is not trivial. We have developed a Windows based Microsoft visual C++ program (Fig. 3). Matlab runs "Simulator_Driver.exe" which opens "Input.dat", calls the EM simulator, opens the proper windows and fills in the necessary information. Simulator_Driver.exe commands the EM simulator to export S-parameters to “Simulator_Output.dat”, which are reformatted to “Output.dat”. We have created Momentum_Driver to drive Momentum [15].

VI. EXAMPLES

The ESMDF algorithm has been tested with $\delta_0 = 0.05$, $\delta_{\min} = 0.005$, $i_{\max} = 10$, and $\varepsilon_1 = 0.005$ on an IBM Aptiva (AMD Athlon, 650 MHz, 384 MB).

Three-Section Microstrip Transformer

This example (Section II) requires 2 iterations (three fine model simulations) to reach the optimal solution in Table II in 17 min. The fine model objective function is shown in Fig. 4. The stopping criterion (13) terminates the algorithm, signifying excellent agreement between the mapped coarse model and fine model. The initial and final solutions are shown in Figs. 5(a) and (b). Table III shows corresponding preassigned parameters.

The final mapped coarse model can be utilized in yield estimation. We assume a uniform distribution with 0.25 mil tolerance on all six geometrical parameters. With 250 outcomes the estimated yield is 78 % compared with 79% using the fine model directly.

HTS Filter (Fig. 6)

The design variables of the HTS bandpass filter (Fig. 6(a)) [16] are the lengths of the coupled lines and the separation between them

$$\boldsymbol{x}_f = [S_1 \; S_2 \; S_3 \; L_1 \; L_2 \; L_3 \,]^T, \boldsymbol{x}_r = [S_1 \; S_2 \; S_3]^T$$

The substrate used is lanthanum aluminate with ε_r= 23.425, H= 20 mil and substrate dielectric loss tangent of 0.00003. The length of the input and output lines is L_0=50 mil and the lines width W= 7 mil. We choose ε_r and H as preassigned parameters, thus $\boldsymbol{x}_0$=[20 mil 23.425]^T. The design specifications are

$$|S_{21}| \leq 0.05 \quad \text{for } \omega \geq 4.099 \text{ GHz and for } \omega \leq 3.967 \text{ GHz}$$

$$|S_{21}| \geq 0.95 \quad \text{for } 4.008 \text{ GHz} \leq \omega \leq 4.058 \text{ GHz}$$

This corresponds to a 1.25% bandwidth. The coarse model consists of empirical models for single and coupled microstrip transmission lines (see Fig. (6b)). All open circuits are considered ideally open. Table IV shows the sensitivity measures for the coarse model responses w.r.t. the preassigned parameters. Fig. 7 depicts significant changes in the coarse model response due to +2% perturbation in both preassigned parameters of each component. The preassigned parameter vector is $\boldsymbol{x} = [\boldsymbol{x}_1^T\ \boldsymbol{x}_2^T\ \boldsymbol{x}_3^T]^T$, where $\boldsymbol{x}_i = [\varepsilon_{ri} \quad H_i]^T$ for i=1, 2, 3. Here

$$\boldsymbol{B}_r = \begin{bmatrix} \mathrm{x} & 0 & 0 \\ \mathrm{x} & 0 & 0 \\ 0 & \mathrm{x} & 0 \\ 0 & \mathrm{x} & 0 \\ 0 & 0 & \mathrm{x} \\ 0 & 0 & \mathrm{x} \end{bmatrix}$$

The fine model is parameterized by Empipe [17] and is simulated by Sonnet's ***em*** [5]. The cell size used is 0.5 mil by 1 mil. All parameter values are rounded to the nearest grid point. Ω_s contains 25 frequencies while Ω_p contains 17. The coarse and fine model responses at the initial solution are shown in Fig. 8, where we notice severe misalignment. The remedy suggested in Section IV managed to get a good solution of (16). The algorithm needs 4 iterations (5 fine model simulations). The time taken is 6.2 hr (one fine model simulation takes 1.2 hr). The fine model objective function is shown in Fig. 9. Table V shows the starting point, the optimal coarse model solution and the final solution. Detailed responses are shown in Fig. 10.

Microstrip Bandstop Filter with Open Stubs (Fig. 11)

The optimization parameters are

$$\boldsymbol{x}_f = [W_1\ W_2\ L_0\ L_1\ L_2\ ]^T, \boldsymbol{x}_r = [W_1\ W_2]^T$$

The width of the middle microstrip line is fixed at W_0= 25 mil. The preassigned parameters are again ε_r and H, with $\boldsymbol{x}_0$=[25 mil 9.4]^T. The dielectric loss tangent is 0.002. The coarse model consists of empirical microstrip lines, Tee-junctions and ideal open circuits (see Fig. 11(b)). The design specifications are

$$|S_{21}| \geq -1 \text{ dB} \quad \text{for } \omega \geq 12 \text{ GHz and for } \omega \leq 8 \text{ GHz}$$

$$|S_{21}| \leq -25 \text{ dB} \quad \text{for } 9 \text{ GHz} \leq \omega \leq 11 \text{ GHz}$$

Because of symmetry we have five components. The sensitivity measures of the coarse model responses w.r.t. the preassigned parameters are given in Table VI. The designated components are taken as # 2, 3, 5. The preassigned parameter vector is $\boldsymbol{x} = [\boldsymbol{x}_2^T \; \boldsymbol{x}_3^T \; \boldsymbol{x}_5^T]^T$, where $\boldsymbol{x}_i = [\varepsilon_{ri} \quad H_i]^T$ for i= 2, 3, 5. Here

$$\boldsymbol{B}_r = \begin{bmatrix} 0 & 0 \\ 0 & 0 \\ \text{x} & 0 \\ \text{x} & 0 \\ 0 & \text{x} \\ 0 & \text{x} \end{bmatrix}$$

Notice that the preassigned parameters of component # 2 are selected not to be functions of $\boldsymbol{x}_r$ (first two rows of $\boldsymbol{B}_r$ are zeros). They are different constants in each iteration. The fine model is analyzed by Momentum [15] and the coarse model by OSA90/hope [13]. We use Momentum_Driver (see Section V). Ω_s contains 35 frequencies while Ω_p contains 17. The algorithm needs 5 iterations (1.5 hr), terminating because the trust region radius reaches its minimum value. The trace of the objective function is shown in Fig. 12. Responses at the initial solution are shown in Fig. 13. Fig. 14 shows a detailed frequency sweep at the solution. The starting point, the optimal coarse model solution and the final solution are given in Table VII.

The fine model was optimized directly using the Momentum minimax optimizer [15], using 17 frequency points, starting at the optimal solution of the coarse model, and converging to the solution in Table VII. Ten hours are required (quadratic interpolation was used). Fig. 15 compares the results of direct Momentum optimization with those of the ESMDF approach.

VII. CONCLUSIONS

We expand the original space mapping technique for circuit design. We deliberately change some preassigned parameters in some of the coarse model components to align the coarse model with the fine model. A mapping is established from the optimization variables to those preassigned parameters. This mapping is sparse and needs only few fine model simulations to be established. Our algorithm calibrates the coarse model w.r.t. the fine model. It updates the mapping and exploits the resulting mapped (enhanced) coarse model with a trust region optimization methodology. Software implementation including interfacing with external EM/circuit simulators is addressed. We have successfully applied our approach to several design problems.

APPENDIX

For filter type responses a rough estimate of the center frequency and bandwidth is as follows. We assume that the response is approximately similar to the pdf curve of a normal distribution. Let the filter response be denoted by $R(\omega)$, where ω is frequency (M points in the range of interest). An approximation to the center frequency μ is given by

$$\mu = (\sum_{i=1}^{M} \omega_i \; R(\omega_i)) / \sum_{i=1}^{M} R(\omega_i) \tag{A.1}$$

Similarly, the bandwidth is approximated by

$$\sigma = 2 \sqrt{(\sum_{i=1}^{M} \omega_i^2 \; R(\omega_i)) / \sum_{i=1}^{M} R(\omega_i) - \mu^2} \tag{A.2}$$

The response R is taken as $|S_{21}|$ for a bandpass filter and $|S_{11}|$ for a bandstop filter. We have to emphasize that although these approximations are rough they are very useful in extracting the preassigned parameters in the case of severe misalignment between coarse and fine models (for example, the HTS filter in Section VI).

ACKNOWLEDGEMENT

The authors thank Dr. J.C. Rautio, President, Sonnet Software, Inc., Liverpool, NY, for making ***em***™ available. The authors also thank Agilent Technologies, Santa Rosa, CA, for making Momentum™ available.

REFERENCES

[1] J.W. Bandler, R.M. Biernacki, S.H. Chen, P.A. Grobelny and R.H. Hemmers, "Space mapping technique for electromagnetic optimization," *IEEE Trans. Microwave Theory Tech.,* vol. 42, 1994, pp. 2536-2544.

[2] J.W. Bandler, M.A. Ismail, J.E. Rayas-Sánchez and Q.J. Zhang, "Neuromodeling of microwave circuits exploiting space mapping technology," *IEEE Trans. Microwave Theory Tech*., vol. 47, 1999, pp. 2417-2427.

[3] M.H. Bakr, J.W. Bandler, K. Madsen, J.E. Rayas-Sánchez and J. Søndergaard, "Space-mapping optimization of microwave circuits exploiting surrogate models," *IEEE Trans. Microwave Theory Tech*., vol. 48, 2000, pp. 2297-2306.

[4] S. Ye and R.R. Mansour, "An innovative CAD technique for microstrip filter design," *IEEE Trans. Microwave Theory Tech*., vol. 45, 1997, pp. 780-786.

[5] ***em***™ Version 4.0b, Sonnet Software, Inc., 1020 Seventh North Street, Suite 210, Liverpool, NY 13088, 1997.

[6] M.H. Bakr, J.W. Bandler, R.M. Biernacki, S.H. Chen and K. Madsen, "A trust region aggressive space mapping algorithm for EM optimization," *IEEE Trans. Microwave Theory Tech.*, vol. 46, 1998, pp. 2412-2425.

[7] N. Alexandrov, J.E. Dennis, Jr., R.M. Lewis and V. Torczon, "A trust region framework for managing the use of approximation models in optimization," *Structural Optimization*, vol. 15, 1998, pp. 16-23.

[8] J. Søndergaard, "Non-linear optimization using space mapping," Masters Thesis, Department of Mathematical Modeling (IMM), Technical University of Denmark (DTU), Lyngby, Denmark, 1999.

[9] J.W. Bandler, S.H. Chen, R.M. Biernacki, L. Gao, K. Madsen and H. Yu, "Huber optimization of circuits: a robust approach," *IEEE Trans. Microwave Theory Tech*., vol. 41, 1993, pp. 2279-2287.

[10] J.W. Bandler, R.M. Biernacki, S.H. Chen, R.H. Hemmers and K. Madsen, "Electromagnetic optimization exploiting aggressive space mapping," *IEEE Trans. Microwave Theory Tech.*, vol. 43, 1995, pp. 2874-2882.

[11] J.W. Bandler, R.M. Biernacki, S.H. Chen and D. Omeragić, "Space mapping optimization of waveguide filters using finite element and mode-matching electromagnetic simulators," *Int. J. RF and Microwave CAE*, vol. 9, 1999, pp. 54-70.

[12] Matlab™, Version 5.3, The MathWorks, Inc., 3 Apple Hill Drive, Natick MA 01760-2098, 1999.

[13] OSA90/hope™ Version 4.0, formerly Optimization Systems Associates Inc., P.O. Box 8083, Dundas, Ontario, Canada L9H 5E7, now Agilent Technologies, 1400 Fountaingrove, Parkway, Santa Rosa, CA 95403-1799.

[14] J.W. Bandler, R.M. Biernacki and S.H. Chen, "Parameterization of arbitrary geometrical structures for automated electromagnetic optimization," *Int. J. RF and Microwave CAE*, vol. 9, 1999, pp. 73-85.

[15] Momentum™ Version 3.5, Agilent Technologies, 1400 Fountaingrove Parkway, Santa Rosa, CA 95403-1799, 1999.

[16] J.W. Bandler, R.M. Biernacki, S.H. Chen, W.J. Getsinger, P.A. Grobelny, C. Moskowitz and S.H. Talisa, "Electromagnetic design of high-temperature superconducting microwave filters," *Int. J. RF and Microwave CAE*, vol. 5, 1995, pp. 331-343.

[17] Empipe™ Version 4.0, formerly Optimization Systems Associates Inc., P.O. Box 8083, Dundas, Ontario, Canada L9H 5E7, now Agilent EEsof EDA, 1400 Fountaingrove, Parkway, Santa Rosa, CA 95403-1799.

TABLE I
RESPONSE SENSITIVITY MEASURES W.R.T. THE PREASSIGNED PARAMETERS OF THE MICROSTRIP TRANSFORMER COARSE MODEL COMPONENTS

Component #	$\hat{S}_i$
1	1.00
2	0.05
3	0.39
4	0.04
5	0.77

TABLE II
VALUES OF THE DESIGN PARAMETERS FOR THE MICROSTRIP TRANSFORMER

Parameter (mm)	Starting point	Optimal coarse model solution	Solution reached by our ESMDF algorithm
W_1	0.40	0.381	0.335
W_2	0.15	0.151	0.136
W_3	0.05	0.042	0.039
L_1	3.00	2.783	2.990
L_2	3.00	3.003	3.079
L_3	3.00	3.085	3.139

TABLE III
VALUES OF THE PREASSIGNED PARAMETERS OF THE MICROSTRIP TRANSFORMER COARSE MODEL DESIGNATED COMPONENTS AT THE INITIAL AND FINAL ITERATIONS

Preassigned parameters	Original value of the preassigned parameters	Preassigned parameters at the final iteration
H_1	25 mil	19.36 mil
H_3	25 mil	20.97 mil
H_5	25 mil	21.48 mil
ε_{r1}	9.7	8.57
ε_{r3}	9.7	9.17
ε_{r5}	9.7	9.31

TABLE IV
RESPONSE SENSITIVITY MEASURES W.R.T. THE PREASSIGNED PARAMETERS OF THE HTS FILTER COARSE MODEL COMPONENTS

Component #	$\hat{S}_i$
1	0.69
2	1.00
3	0.30

TABLE V
VALUES OF THE DESIGN PARAMETERS FOR THE HTS FILTER

Parameter (mil)	Starting point	Optimal coarse model solution	Solution reached by our ESMDF algorithm
S_1	20.0	20.76	19.0
S_2	100	108.46	78.0
S_3	100	101.80	80.0
L_1	190	172.27	178.5
L_2	190	213.83	201.5
L_3	190	172.74	177.5

TABLE VI
RESPONSE SENSITIVITY MEASURES W.R.T. THE PREASSIGNED PARAMETERS OF THE MICROSTRIP OPEN STUB FILTER COARSE MODEL COMPONENTS

Component #	$\hat{S}_i$
1	0.14
2	0.64
3	0.84
4	0.19
5	1.00

TABLE VII
VALUES OF THE DESIGN PARAMETERS FOR THE MICROSTRIP OPEN STUB FILTER

Parameter (mil)	Starting point	Optimal coarse model solution	Solution reached by our ESMDF algorithm	Solution obtained by direct optimization
W_1	5.00	3.79	3.80	3.70
W_3	10.0	10.25	10.16	9.89
L_0	120	124.23	124.78	117.50
L_1	120	131.60	124.61	125.05
L_2	120	115.89	107.48	110.03

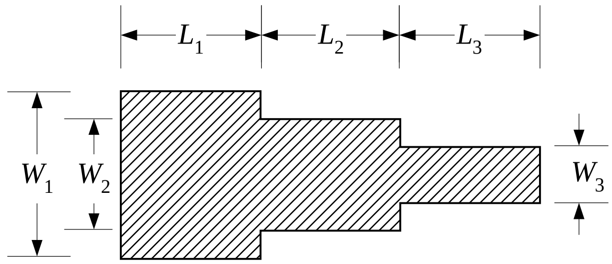

(a)

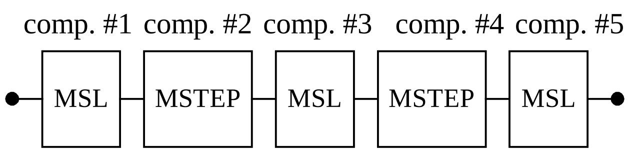

(b)

Fig. 1. Three-section microstrip transformer: (a) the physical structure; (b) the coarse model.

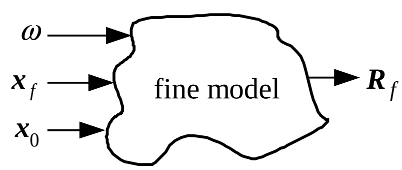

(a)

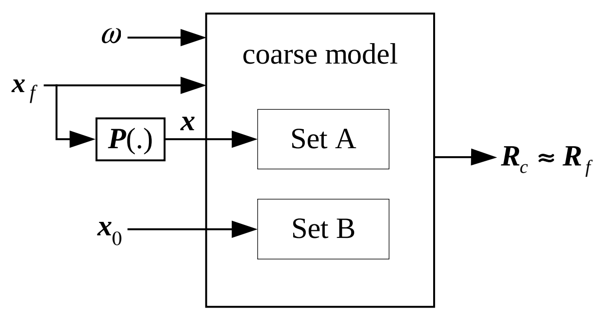

(b)

Fig. 2. Changing the preassigned parameters in some of the coarse model components (the components in Set A) results in aligning the coarse model (b) with the fine model (a).

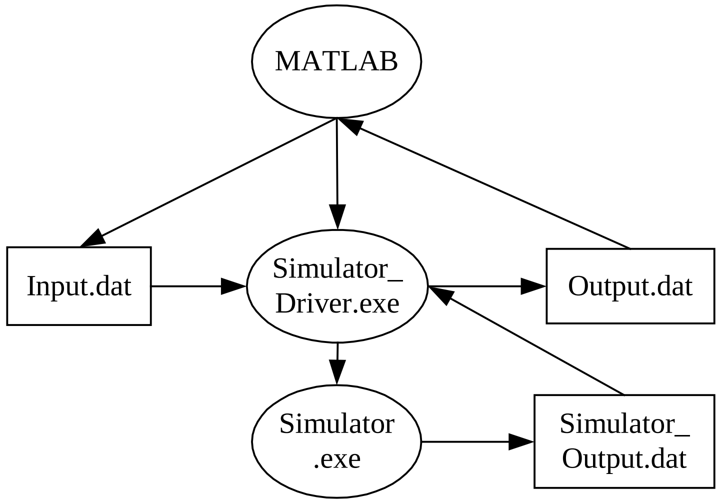

Fig. 3. Driving EM/circuit simulators from inside Matlab.

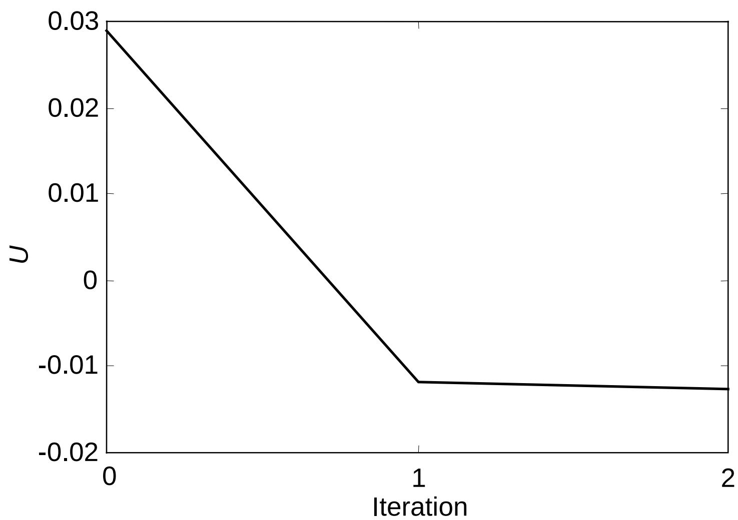

Fig. 4. The objective function of the microstrip transformer fine model.

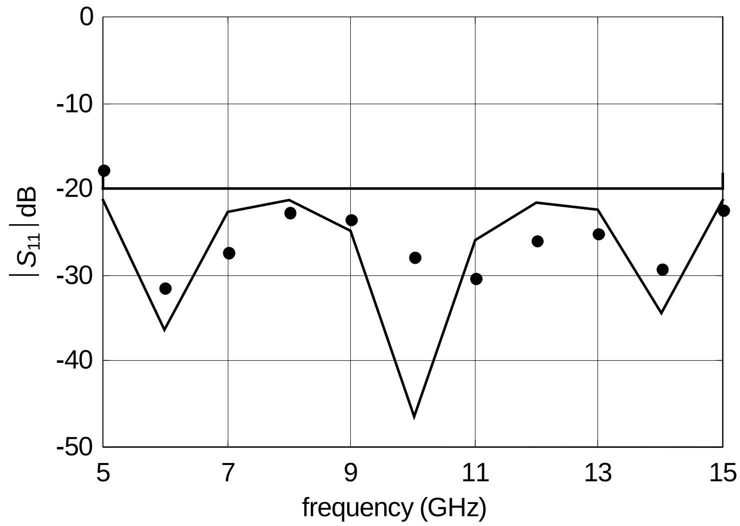

(a)

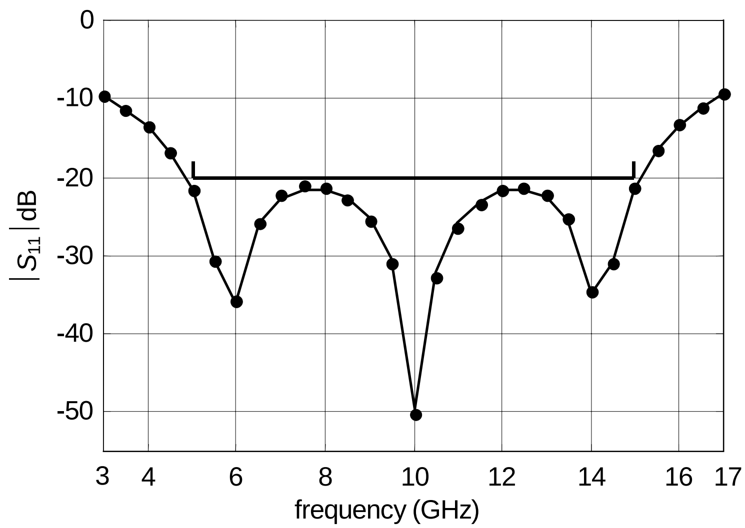

(b)

Fig. 5. The fine (•) and mapped coarse model (—) responses of the microstrip transformer: (a) at the initial solution; (b) at the final solution (detailed frequency sweep).

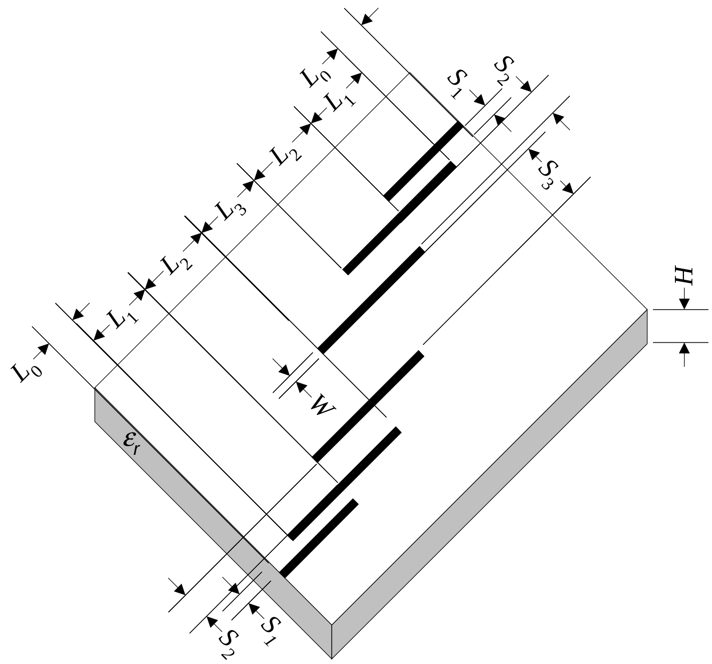

(a)

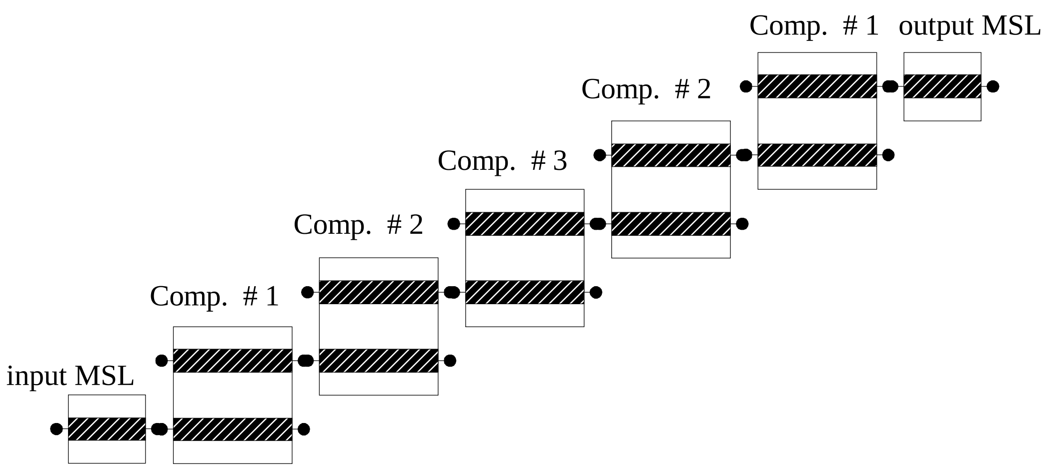

(b)

Fig. 6. The HTS filter: (a) the physical structure; (b) the coarse model.

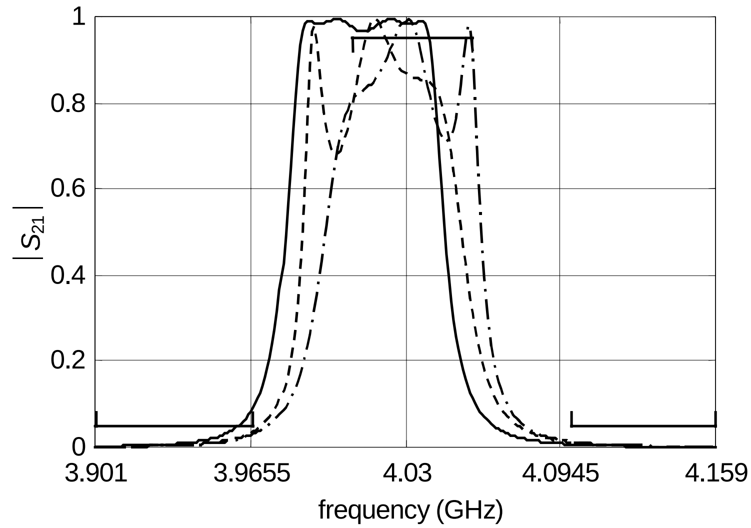

Fig. 7. The coarse model response resulting from 2% perturbation in the preassigned parameters of: (a) the first component (–·–·–); (b) the second component (—); (c) the third component (- - -).

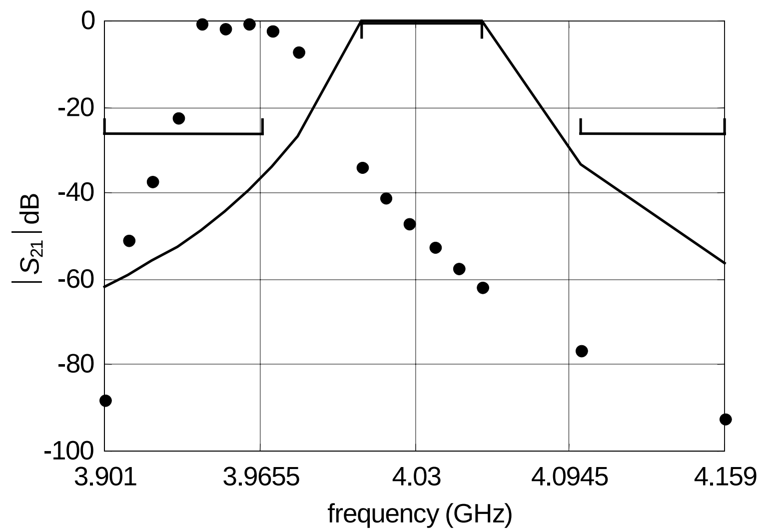

Fig. 8. The Sonnet ***em*** fine model response (••) and the coarse model response (—) of the HTS filter at the initial solution.

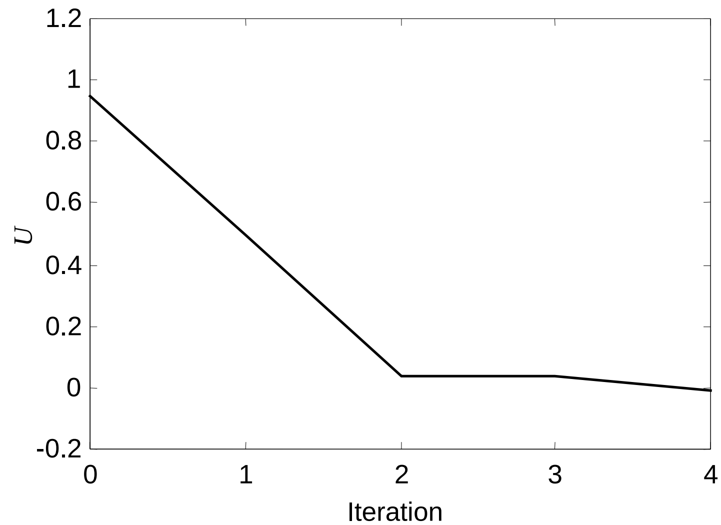

Fig. 9. The objective function of the HTS filter fine model.

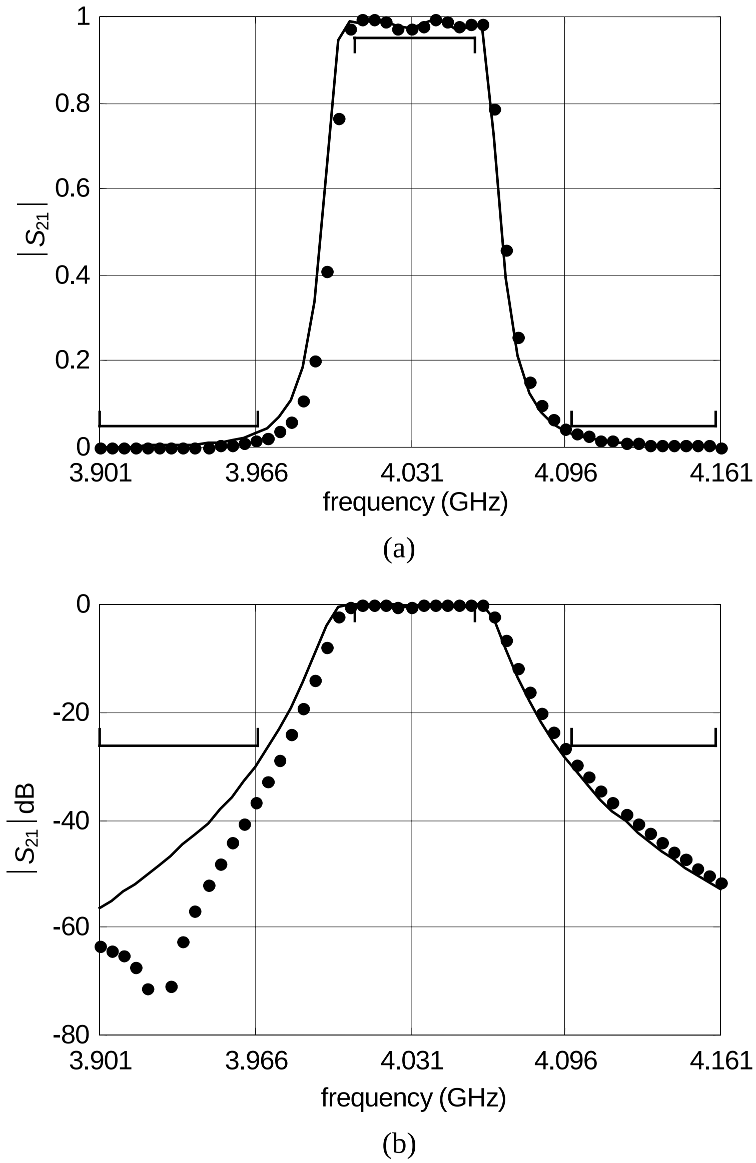

Fig. 10. Detailed frequency sweep of the fine and coarse model responses of the HTS filter at the final solution: (a) $|S_{21}|$; (b) $|S_{21}|$ in decibels.

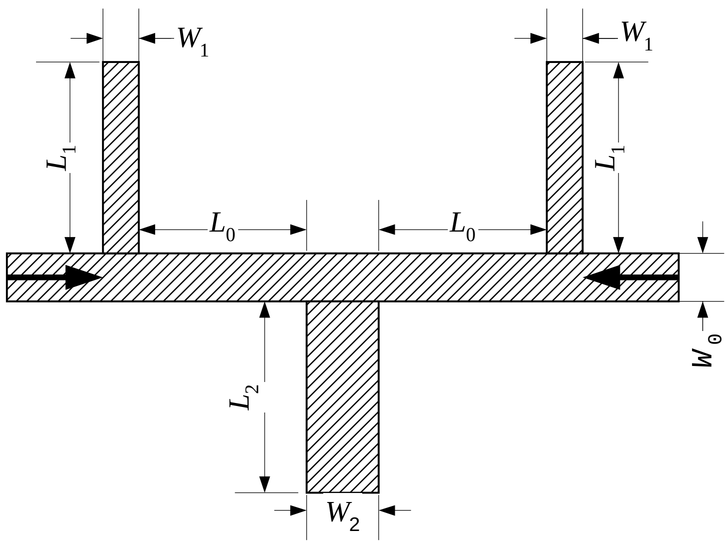

(a)

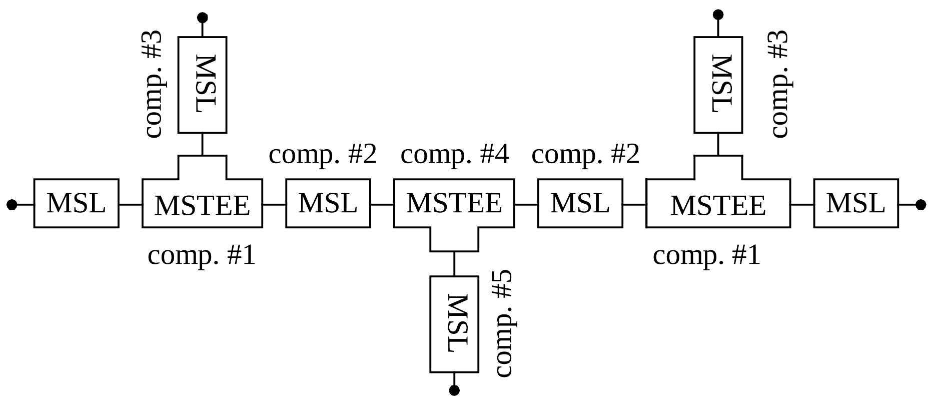

(b)

Fig. 11. Microstrip bandstop filter with open stubs: (a) the physical structure; (b) the coarse model.

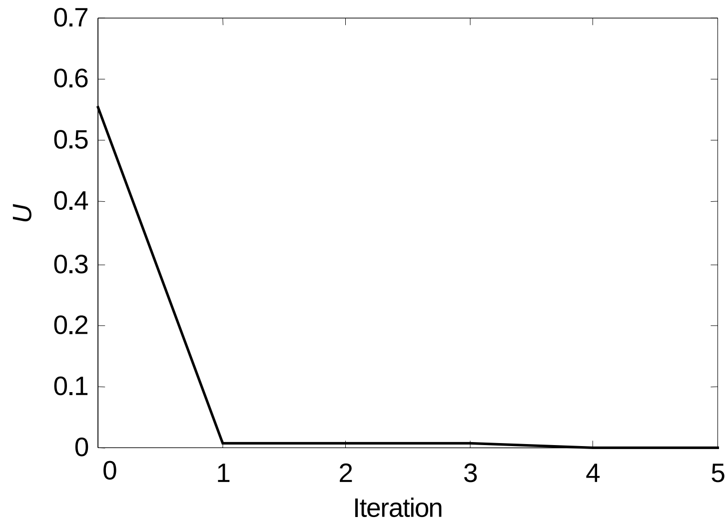

Fig. 12. The objective function of the open stub filter fine model.

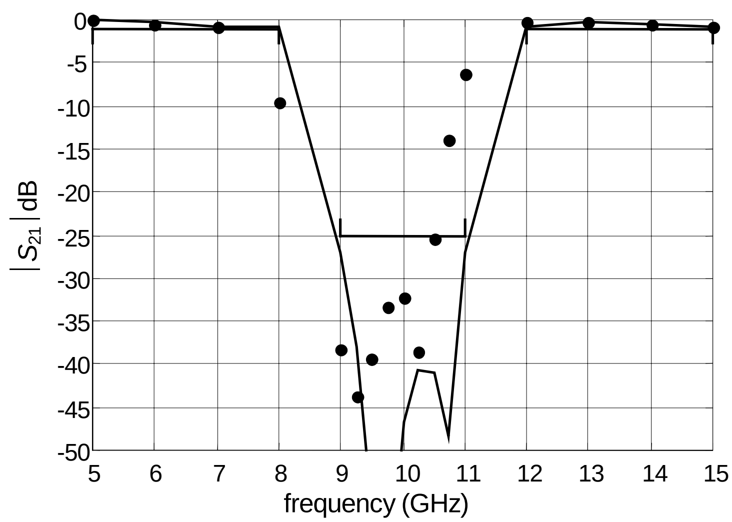

Fig. 13. The fine model response (••) versus the coarse model response (—) of the open stub filter at the initial solution.

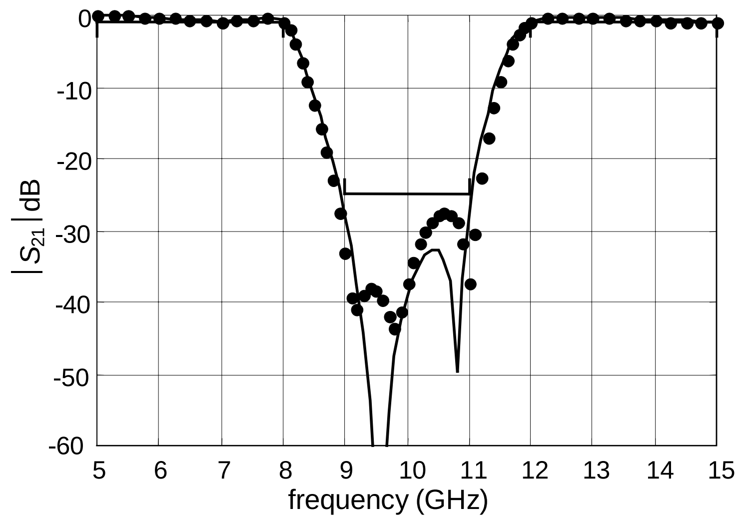

Fig. 14. Detailed frequency sweep of the fine and coarse model responses of the open stub filter at the final solution.

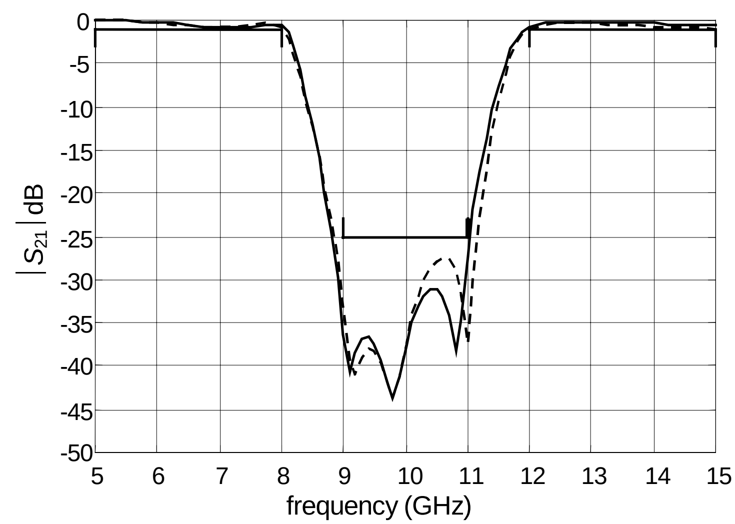

Fig. 15. The fine model responses of the open stub filter at the solution obtained by direct Momentum optimization (—) and by our ESMDF algorithm (----).